The Korean Journal of Applied Statistics (2009)
22(1), 221–235

Statistical Modeling on Weather Parameters to Develop Forest Fire Forecasting System

Manish Trivedi[1] · Manoj Kumar[2] · Ripunjai Shukla[3]

[1]Dept. of Applied Mathematics, Birla Institute of Technology;
[2]Dept. of Applied Mathematics, Birla Institute of Technology;
[3]Dept. of Applied Mathematics; Birla Institute of Technology

(Received November 2008; accepted December 2008)

Abstract

This manuscript illustrates the comparative study between ARIMA and Exponential Smoothing modeling to develop forest fire forecasting system using different weather parameters. In this paper, authors have developed the most suitable and closest forecasting models like ARIMA and Exponential Smoothing techniques using different weather parameters. Authors have considered the extremes of the Wind speed, Radiation, Maximum Temperature and Deviation Temperature of the Summer Season form March to June month for the Ranchi Region in Jharkhand. The data is taken by own resource with the help of Automatic Weather Station. This paper consists a deep study of the effect of extreme values of the different parameters on the weather fluctuations which creates forest fires in the region. In this paper, the numerical illustration has been incorporated to support the present study. Comparative study of different suitable models also incorporated and best fitted model has been tested for these parameters.

Keywords: ARIMA, Exponential Smoothing, temperature, maximum, minimum, wind speed, radiation.

1. Introduction

Forest fires that are natural or man made play a significant role in ecosystem dynamics. Recurrent fire decreases the green cover through prevention of regeneration and leads to the slow death of the forest. It also increases erosion and alters the physical and chemical properties of the soil, converting organic ground cover to soluble ash and modifying the microclimate through the removal of overhead foliage. Weather is one of the most significant factors in determining the spread rate and intensity of fires. Two of the most important weather parameters are wind and relative humidity. In general, the higher the wind speed and lower the relative humidity the greater the potential and intensity of fires. Windy conditions will help in spreading the fire upwind while lower humidity's will quickly dry out vegetation such as leaves and branches, making wildfires harder to contain.

This work is supported by NRDMS, Department of Science and Technology, New Delhi.
[1]Corresponding author: Dept. of Applied Mathematics, Birla Institute of Technology, Mesra, Ranchi-835215, India. Email: manish_trivedi1976@yahoo.com

1.1. Existing fire models

Previous authors have taken several approaches to modeling fires in landscapes. The most detailed approach is based on Rothermel's (1972) physical model of fire spread. Rothermel's model was developed for forest fire managers to predict fire behavior. It is a physical model, based on an application of the law of conservation of energy to a unit volume of fuel. Because the fuel bed is assumed to be continuous and contiguous to the ground, Rothermel's model is not intended for use in predicting the behavior of crown fires or spotting behavior. Required inputs for Rothermel's model include fuel characteristics, such as fuel loading, fuel depth, fuel particle surface area-to-volume ratio, heat content, particle density, moisture content, moisture of extinction, and mineral content; slope; and wind speed. Equations are then used to predict the rate of spread and intensity of the flame front. Frandsen and Andrews (1979) used Rothermel's equations to predict fire behavior in non-uniform fuels. They expressed the fuel types as an array of cells. The model produced a series of probability distributions of fire-spread rates and intensity. Burrows (1988) expanded on the idea of using Rothermel's model to predict spread across a grid of non-uniform fuels. The study simulated vegetation patterns in time and space, rather than overall distributions of fire behavior. The spread of fire from a burning cell to a neighboring cell was modeled as a stochastic process, with the spread probability conditioned on the spread rate calculated using Rothermel's model. Fuel types and slopes were allowed to vary from cell to cell, but weather conditions and fuel drying rates were assumed homogeneous throughout the landscape. Weather conditions at the time of each fire were selected at random from weather station records. Flammability was assumed to increase predictably as the vegetation grew back after a burn.

1.2. Modeling fire pattern directly

The need to make models discrete in space and time relates to the arguments suggested by hierarchy theory for appropriate choice of scale. In this model, we were interested in landscape patterns that result from fires, not the short term dynamics of a single fire front as it occurs. Other approaches to modeling disturbance in landscape focus more directly on the patterns, and less on the physics, of the disturbance event itself. Baker *et al.* (1991) describe a model that expresses a landscape disturbance regime as a distribution of patch sizes. The parameters of the distribution (negative exponential) vary under the influence of weather and landscape attributes, such as the time since last disturbance. Agee and Flewelling (1983) developed a fire-cycle model for the Olympic National Park, based on statistical relationships, in which fire size was expressed as a function of droughtiness. Statistically, modelling a disturbance regime requires knowledge of the distribution of various attributes of the disturbance regime in space and time (Baker 1992). The size distributions for fires have been described as negative exponential (van Wagtentonk, 1986; Baker, 1989b) or power function (Minnich, 1983) distributions. Several investigators have mapped historical fire patterns and estimated the proportion of study areas burned over a time-series of years (Heinselman, 1973; Romme, 1982; Clark, 1990). The distribution of shapes of disturbance events should also be considered. Anderson (1983) fit a double ellipse model to wind-driven fire size and shape. His model has been incorporated into the Rothermel *et al.* (1986) model to predict fire perimeter, area, and spread patterns. In a simulation model of fire spread in nonuniform fuels, Green (1983) found that fire shapes were irregular and often non-elliptical. The irregularity of fire shapes due to variations in local topography and weather in Sierra Nevada red fir forests has been observed by Kilgore (1971). A mapping of historical fires in northwestern Minnesota also suggested irregular, patchy fires (Clark 1990). Temporal distributions of fire events must also be understood if fire patterns are to be modeled statistically. The distribution of fire return intervals has been empirically fit to a Weibull distribution (Johnson and Van Wagner, 1985), which changes in form over time with climatic shifts (Clark, 1989; Swetnam, 1993). Many field studies of fire return intervals only report a mean and a range (*e.g.* Martin, 1982; Agee and Flewelling, 1983), which are inadequate statistics for deriving an asymmetrical distribution. Swetnam (1993) found that fire size in giant sequoia groves decayed exponentially with fire frequency. Finally, models must reflect the spatial arrangement of fires of varying intensity. Fire effects such as tree mortality and removal of biomass are affected by scorch height, which is a function of fire intensity (Brown *et al.*, 1985; Ryan and Reinhardt, 1988). Both fire probability (Fowler and Asleson, 1984) and intensity (Kilgore, 1973) vary considerably according to site characteristics.

1.3. Statistical fire modeling

Various statistical methods have been used to describe and model vegetation patterns. Logistic regressions, which include neighborhood effects, have been fit to fire probability data in the San Jacinto Mountains (Chou *et al.*, 1990). These models are generally empirical and often ignore much of that is known about the underlying physical and biological processes. In many problems the formulation of the prior environmental knowledge in terms of the parameters of the statistical model is of fundamental importance as is the need to evaluate model and prediction uncertainties. Point pattern analysis (Greig-Smith, 1964; Pielou, 1977) has been used to describe levels of contagion in plant communities (Bonnicksen and Stone, 1982). As the name point pattern suggests, these analyses are typically used to test departure from random dispersion at the scale of individual trees. Geostatistical methods have been used to simulate spatial patterns in ecology (Rossi *et al.*, 1993), by expressing spatial auto-correlation as a function of distance. The largest study of the statistics of fire pattern to date covered an 85-year fire record for seven National Forests in the Sierra Nevada (McKelvey and Busse, 1996). Using logistic regression methods, McKelvey and Busse (1996) linked fire occurrence to topographic features, principally elevation. In addition, McKelvey and Busse (1996) described the size-distribution of fires, and demonstrated their correlation to seasonal weather patterns both at the scale of the entire Sierra Nevada and within the context of local topography. Different models have been extensively used in practice for forecast economics time series, inventory and sales model and generalization of the exponential weighted moving average process (Makridakis *et al.*, 2003). Meese and Geweke (1982) have discussed the methods of identifying univariate models. Among the others Quenouille (1949), Ljung and Box (1978) and Pindyck and Rubinfeld (1981) have also emphasized the use of ARIMA models. As one would expect, this is quite a difficult model to be developed and applied as it involves transformation of the variable, identification of the model, estimation through nonlinear method, verification of the model and derivation of the forecasts (Box and Jenkins, 1976).The unit of ARIMA models lies in their ability to reveal complex structures of temporal interdependence in time series. It has also been shown that ARIMA models are highly efficient in short term forecasting (Ljung and Box, 1978).

2. Methodology

The time series modeling assumes that a time series is a combination of a pattern and some random error. The goal is to separate the pattern from the error by understanding the pattern's trend, its long term increase and decrease and its seasonality. Several methods of time series forecasting are available such as the Autoregression, Moving Averages, Autoregressive Integrated Moving Average(ARIMA) methos, Linear Regression with time, Exponential Smoothing, *etc.* This study concentrates on ARIMA and Exponential Smoothing technique as applied to time series weather parameters such as maximum temperature, wind speed *etc.*

2.1. Exponential Smoothing model

This is also known as simple exponential smoothing. Simple smoothing is used for short-range forecasting, usually just one step ahead into the future. The model assumes that the data fluctuates around a reasonably stable mean (no trend or consistent pattern of growth). The specific formula for simple exponential smoothing is (Pankratz, 1983)

$$S_t = \alpha X_t + (1 - \alpha) S_{t-1}, \tag{2.1}$$

where X_t is the observation at time t, S_t is the forecasted value at time t and α is the damping factor having the range $0 < \alpha < 1$.

When applied recursively to each successive observation in the series, each new smoothed value (forecast) is computed as the weighted average of the current observation and the previous smoothed observation; the previous smoothed observation was computed in turn from the previous observed value and the smoothed value before the previous observation, and so on.

2.2. Initial value

The initial value of S_t plays an important role in computing all the subsequent values. Setting it to x_1 is one method of initialization. Another possibility would be to average the first four or five observations. The smaller the value of α, the more important is the selection of the initial value of S_t.

2.3. Testing the homogeneity of error variance(MSE)

Bartlett test carried out to check the homogeneity of Error Mean Sum of Square(MSE) that whether they are homogeneous or not at various values of damping factor α. The test statistic of Bartlett test is given by the following formula

$$\chi^2 = \frac{\sum_{i=1}^{k} \left(v_i \log \frac{S^2}{S_i} \right)}{1 + \frac{1}{3(k-1)} \left(\sum_{i=1}^{k} \frac{1}{v_i} - \frac{1}{v} \right)}, \tag{2.2}$$

where

$$S^2 = \frac{\sum_{i=1}^{k} v_i S_i^2}{\sum_{i=1}^{k} v_i} = \frac{\sum_{i=1}^{k} v_i S_i^2}{v}, \quad \sum_{i=1}^{k} v_i = v.$$

In the above expression S_i^2 is the i^{th} MSE and v_i is the corresponding degree of freedom. The test statistics follows χ^2 distribution with $(k-1)$ degree of freedom.

2.4. Autoregressive integrated moving average model

A time series is a set of values of a continuous variable $Y\,(Y_1, Y_2, \ldots, Y_n)$, ordered according to a discrete index variable $t\,(1, 2, \ldots, n)$. However, it must be clearly stated that this direct reference to time is not required; a different meaning can be attributed to the index variable, provided that it is able to order the Y values. In general, in a given time series the following can be recognizing and separated

- A regular, long-term component of variability, termed trend that represent the whole evolution pattern of the series.
- Stationarity is a critical assumption of time series analysis, stipulating that statistical descriptors of the time series are invariant for different ranges of the series. Weak stationarity assumes only that the mean and variance are invariant.
- A regular short term component whose shape occurs periodically at intervals of s lags of the index variable, currently known as seasonality, because this term is also derived by application in economics.
- An AR (p) *i.e.* autoregressive component of order p which relates each value $Z_t = Y_t$ (trend and seasonality) to the p previous Z values, according to the following linear relationship

$$Z_t = \phi_1 Z_{t-1} + \phi_2 Z_{t-2} + \cdots + \phi_p Z_{t-p} + \epsilon_i, \tag{2.3}$$

where $\phi_i\,(i = 1, \ldots, p)$ are parameters to be estimated and ϵ_i is the residual terms.

A MA(q), *i.e.* moving average component of q order, which relates each Z_t values to the q residuals of the q previous Z estimates

$$Z_t = \epsilon_t - \theta_1 \epsilon_{t-1} - \theta_2 \epsilon_{t-2} - \cdots - \theta_q \epsilon_{t-q}, \tag{2.4}$$

where $\theta_i\,(i = 1, \ldots, p)$ are parameters to be estimated. According to Box-Jenkins (Agee and Flewelling, 1983) a highly useful operator in time series theory is lag or backword linear operator (B) defined by $BZ_t = Z_{t-1}$.

Consider the result of applying the lag operator twice a series:

$$B(BZ_t) = BZ_{t-1} = Z_{t-2}.$$

Such a double indication is indicated by B^2 and in general for any integer k, it can be written $B^k Z_t = Z_{t-k}$. By using the backword operator, Equation (2.1) can be rewritten as

$$Z_t - \phi_1 Z_{t-1} - \phi_2 Z_{t-2} - \cdots - \phi_p Z_{t-p} - \epsilon_t = \phi(B) Z_t \tag{2.5}$$

where $\phi(B)$ is the autoregressive operator of order p defined by

$$\phi(B) = 1 - \phi_1 B - \phi_2 B^2 - \cdots - \phi_p B^p.$$

Similarly, Equation (2.3) can be written as

$$Z_t = \epsilon_t - \theta_1 \epsilon_{t-1} - \theta_2 \epsilon_{t-2} - \cdots - \theta_q \epsilon_{t-q} = \theta(B) \tag{2.6}$$

where $\theta(B)$ indicated the moving average operator of q order defined by

$$\theta(B) = 1 - \theta_1 B - \theta_2 B^2 - \cdots - \theta_q B^q.$$

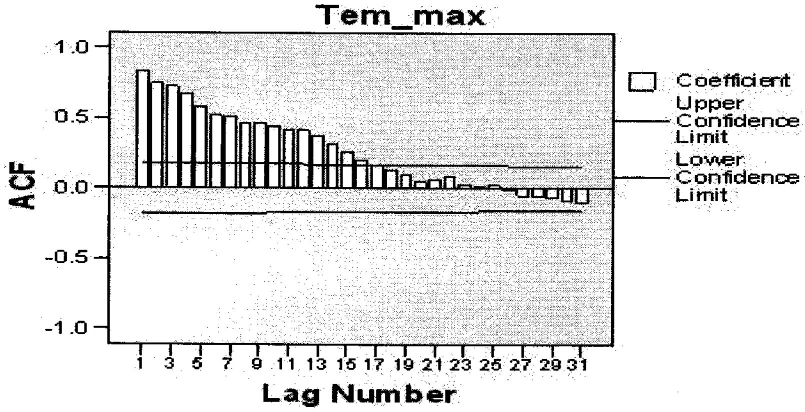

Figure 3.1. Correlogram of maximum temperature before transformation

The autoregressive(AR) and Moving Average(MA) components can be combined in an autoregressive moving average ARMA(p, q) model

$$Z_t = \phi_1 Z_{t-1} + \phi_2 Z_{t-2} + \cdots + \phi_p Z_{t-p} + \epsilon_i - \theta_1 \epsilon_{t-1} - \theta_2 \epsilon_{t-2} - \cdots - \theta_q \epsilon_{t-q}$$

or in lag operator from

$$(1 - \phi_1 B - \phi_2 B^2 - \cdots - \phi_p B^p) Z_t = (1 - \theta_1 B - \theta_2 B^2 - \cdots - \theta_q B^q)\epsilon_t.$$

Finally,

$$\Phi(B) Z_t = \theta(B)\epsilon_t. \tag{2.7}$$

The value of AR (ϕ) term always should be keep in the equation with positive sign and negative sign attached to MA (θ_1) which is merely a convention. It makes no difference whether we use a negative or positive sign. There is one more condition about the coefficients of model that they should not exceed unity which is known as invertibility condition (Agee and Flewelling, 1983). From the tentative ARIMA models the best models were selected which has minimum MSE, Akike Information Criterion(AIC), Schwartz Bayesian Criterion(SBC) (Baker, 1989a) values and follow the assumptions of residual.

3. Modeling of Parameters

3.1. Modeling of maximum temperature

3.1.1. ARIMA modeling approach Data series found to be non-stationary because its autocorrelation function(acf) did not sharply damping towards zero so that transformation is required by taking difference $d = 1$. Now the data series converted in stationary form as the Figure 2(a) & (b) revealed. The Figure 3.2(a) indicated that *acf* cut-off occurring at lag first and in Figure 3.2(b) *pacf*s cut-off occurring at lag first and second so from the ARIMA family fitted models will be for all values of $p = 0, 1, d = 1$ and $q = 0, 1, 2$ *i.e.* fitted model from ARIMA family are ARIMA$(1, 1, 0)$, ARIMA$(1, 1, 1)$, ARIMA$(0, 1, 1)$, ARIMA$(0, 1, 2)$, ARIMA$(1, 1, 2)$ which are given in Table 3.1.

The above table indicates that all the models have their coefficients significant at 5percent probability level excepting to ARIMA$(0, 1, 2)$. But the constants are non-significant for all the models,

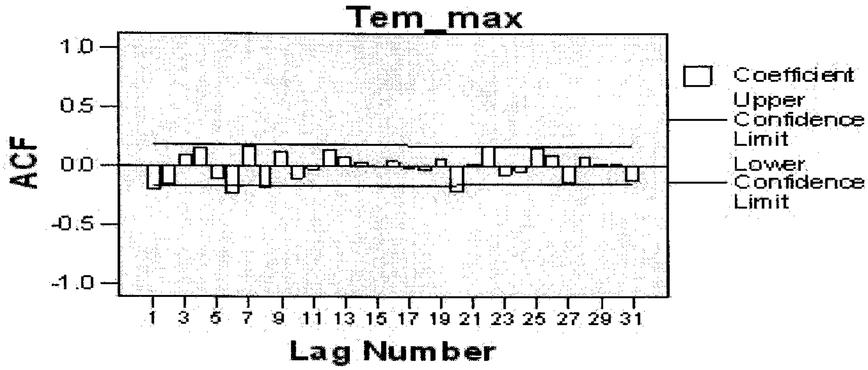

(a) Correlogram of Maximum Temperature at different lags before transformation

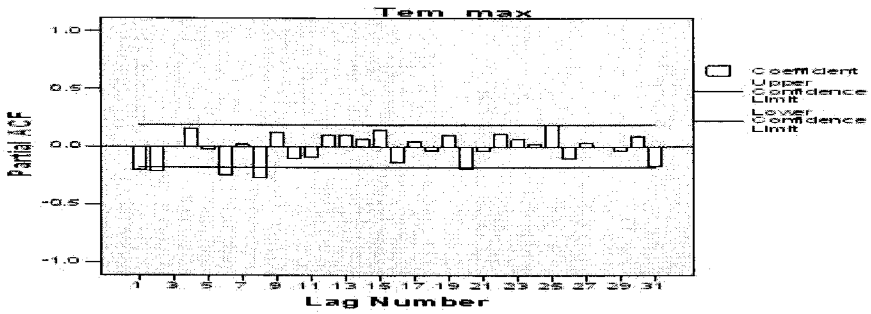

(b) Correlogram of Maximum Temperature at different lags after transformation

Figure 3.2

Table 3.1. Fitted ARIMA models for Maximum Temperature data

Model	AR(Φ)	MA(θ)	Constant	AIC	SBC	MSE
ARIMA(1,1,0)	−0.207*	--	−0.002ns	498.22	504.79	3.658
ARIMA(1,1,1)	.448*	.742*	−0.004ns	496.20	504.56	3.563
ARIMA(0,1,1)		.302*	−0.002ns	495.44	505.02	3.573
ARIMA(0,1,2)		.248*, .143	−0.001ns	495.59	503.96	3.547
ARIMA(1,1,2)	.785*	.559*, .355*	−0.002ns	493.09	504.24	3.453

* Significant at 5 percent probability level, ns- non-significant

so that one can easily say that there is no role of constants in any model. The best model will be chosen on the basis of significant coefficients and least values of AIC(Akike's Information Criterion), SBC(Squartz-Bayesian Criterion) and Mean Square of Error(MSE). ARIMA(1,1,2) satisfies all the assumptions which are considered for this experiment, so it will be our candidate model from the fitted model to predict the trend of maximum temperature. The captured trend by ARIMA(1,1,2) is indicated in the Figure 3.3 given below.

The fitted model for maximum temperature

$$\hat{Y}_t = C + 0.785Y_{t-1} - 0.559\epsilon_{t-1} - 0.355\epsilon_{t-2} + \epsilon_i.$$

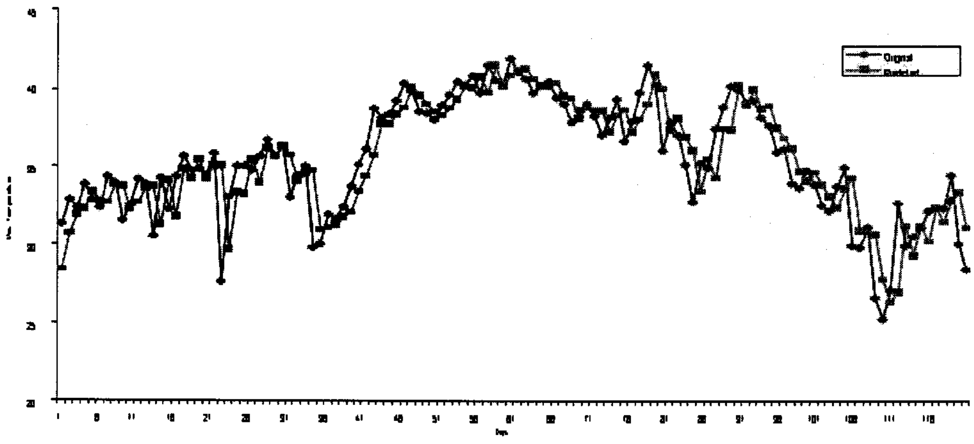

Figure 3.3. Observed and predicted values of maximum temperature through ARIMA(1, 1, 2)

Table 3.2. Smoothing technique for Maximum Temperature Data

$\alpha = 0.9$			$\alpha = 0.8$			$\alpha = 0.7$		
MSE	K-S Test	Run Test	MSE	K-S Test	Run Test	MSE	K-S Test	Run Test
4.001	0.112*	1.025ns	3.892	0.113*	−0.662ns	3.837	0.112*	0.083ns
Bartlett Test for MSE			Not Required due to failure of Normality of residuals					

Table 3.3. ARIMA modeling of deviation temperature

Model	AR(Φ)	MA(θ)	Constant	AIC	SBC	MSE
ARIMA(1, 1, 0)	−0.385*	--	−0.085	543.19	548.75	5.521
ARIMA(1, 1, 1)	0.294*	0.829*	−0.093ns	531.83	540.17	4.955
ARIMA(0, 1, 1)	--	0.617*	−0.090ns	534.48	540.04	5.118
ARIMA(0, 1, 2)	--	.565*, .169ns	−0.094ns	533.09	541.42	5.008
ARIMA(1, 1, 2)	−0.894*	−.494ns, 0.506ns	−0.089ns	533.59	544.70	4.924
ARIMA(2, 1, 0)	−0.462*, −0.206*		−0.870ns	540.21	548.54	5.336

3.1.2. Exponential Smoothing approach The Exponential Smoothing model had also been tried for fitting on the Maximum Temperature data but it could not pass the randomness test as well as the normality test. The results are given in the Table 3.2. The MSE is very large and greater than the ARIMA(1, 1, 2) Model, which is the best fitted model for the extreme values of Maximum Temperature. Bartlett's test for MSE is not operated on the Exponential Smoothing model because of its failure to randomness test and normality test of residuals.

3.2. Modeling of deviation temperature

3.2.1. ARIMA modeling approach The ARIMA family models had also been tried for fitting on the Deviation Temperature data. According to the *acf* and *pacf* criteria the candidate models are ARIMA(1, 1, 0), ARIMA(1, 1, 1), ARIMA(0, 1, 1), ARIMA(0, 1, 2), ARIMA(1, 1, 2) and ARIMA(2, 1, 0). Among these models ARIMA(2, 1, 0) has its coefficients significant and lower value if AIC And BIC and easily fulfill the condition of invertibility for model coefficients which is illustrated by Table 3.3.

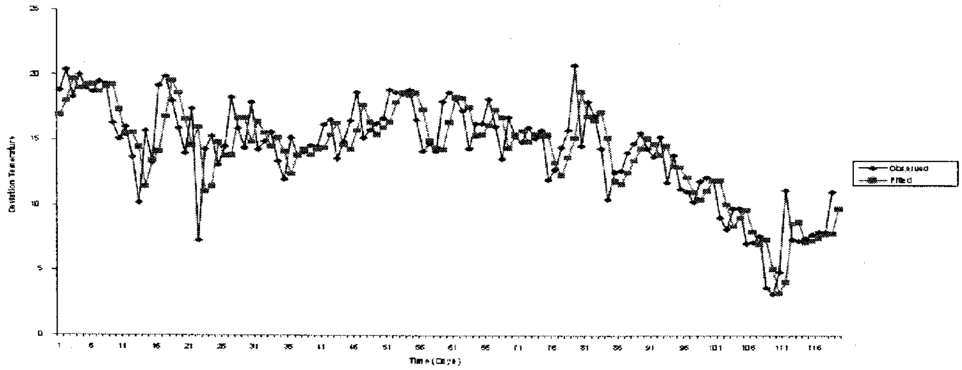

Figure 3.4. Observed and predicted deviation temperature through ARIMA(2, 1, 0) model

Table 3.4. Fitted Exponential Smoothing models for deviation temperature data

$\alpha = 0.7$			$\alpha = 0.8$			$\alpha = 0.9$		
MSE	K-S Test	Run Test	MSE	K-S Test	Run Test	MSE	K-S Test	Run Test
5.472	0.054ns	−.214ns	5.681	0.063ns	.265ns	5.978	0.071ns	.520ns
Bartlett Test for MSE			0.109ns(PASS)					

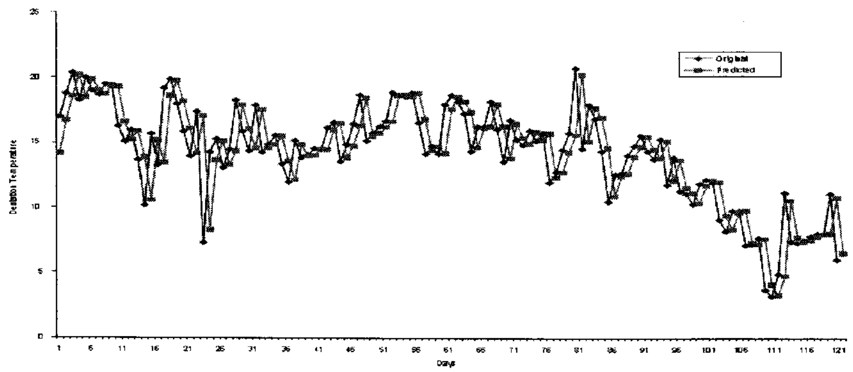

Figure 3.5. Observed and predicted deviation temperature through Exponential Smoothing technique

3.2.2. Smoothing approach The simple exponential smoothing technique is adopted to get the trend of deviation temperature. It is fitted on the various values of α (0.7, 0.8 and 0.9) and the best were adopted on the Goodness of Fit (K-S test), Run test and leas value of MSE. Here in this case all the models were fulfilled the all required criteria but MSE slightly vary as α increase towards higher value, so Bartlett test is used to test the homogeneity of MSE which was successfully pass as indicated in the Table 3.2.

The graph between observed and predicted values was observed very much closer when increasing toward higher values of α.

The fitted model for deviation temperature

$$\hat{F}_t = 0.9Y_{t-1} + 0.1F_{t-1}.$$

Table 3.5. Fitted ARIMA modeling of wind speed

Model	AR(Φ)	MA(θ)	Constant t	AIC	SBC	MSE
ARIMA(1,1,0)	−.515*	−.797*	2.319*	229.79	238.18	.381
ARIMA(2,0,1)	−.523*, .039*	−.819*	2.318*	231.69	242.88	.384
ARIMA(0,0,1)						
ARIMA(0,0,2)		−.317*, .124ns	2.319*	233.32	241.71	.392
ARIMA(1,0,2)	.886*	.635*, .158ns	2.305*	235.87	247.06	.398
ARIMA(2,0,0)	.223*, −.002ns	--	2.318*	235.82	244.21	.401

Table 3.6. Fitted Exponential Smoothing models for deviation temperature data

$\alpha = 0.7$			$\alpha = 0.8$			$\alpha = 0.9$		
MSE	K-S Test	Run Test	MSE	K-S Test	Run Test	MSE	K-S Test	Run Test
.517	0.073ns	1.370ns	.553	0.066ns	1.005ns	0.593	0.073ns	1.735ns
Bartlett Test for MSE				0.244ns(PASS)				

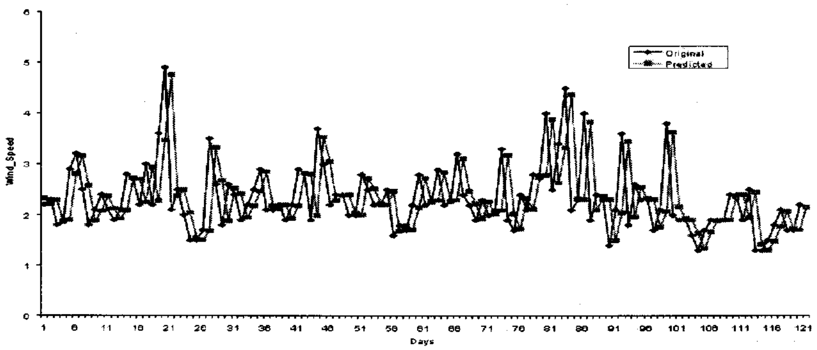

Figure 3.6. Observed and predicted wind speed through Exponential Smoothing technique

3.3. Modeling of wind speed

3.3.1. Arima modeling approach The ARIMA models had also been tried for fitting on the Wind Speed data but it could not pass the invertibility conditions for coefficients of ARIMA models. The results are given in the Table 3.5. The MSE are large and greater than the Exponential Smoothing model which is found to be the best fitted model for the Extreme values of the Wind Speed. The ARIMA Models fitted on the Wind Speed data failed to Bartlett's Test for MSE.

3.3.2. Exponential Smoothing approach Like the deviation temperature, simple exponential smoothing technique is adopted to get the trend for wind speed data. It is fitted on the various values of α(0.7, 0.8 and 0.9) and the best were adopted on the Goodness of Fit (K-S test), Run test and least value of MSE. Here in this case all the models were fulfilled the all required criteria but MSE slightly vary as α increase towards higher value, so that Bartlett test is used to test the homogeneity of MSE which was successfully pass as indicated in the Table 3.6.

Although the MSE values slightly increase fractionally as α increase but the graph between observed and predicted values was observed very much closer when increasing toward higher values of α. **The fitted model for Wind Speed**

$$\hat{F}_t = 0.9Y_{t-1} + 0.1F_{t-1}.$$

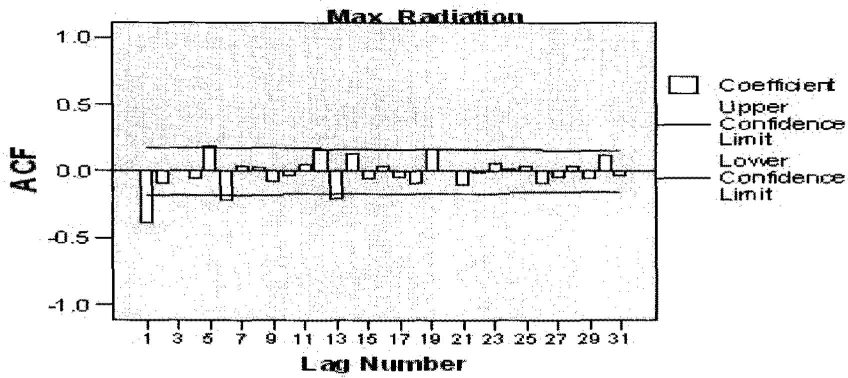

(a) Correlogram of maximum solar radiation at different lags before transformation

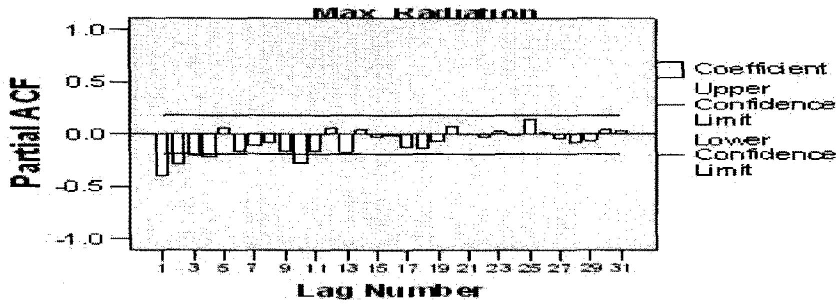

(b) Correlogram of maximum solar radiation at different lags after transformation

Figure 3.7

Table 3.7. Fitted ARIMA models for Maximum Solar Radiation data

Model	AR(Φ)	MA(θ)	Constant	AIC	SBC	MSE
ARIMA(1, 1, 0)	−0.392*	- -	0.448ns	1483.2	1487.8	13411.4
ARIMA(1, 1, 1)	0.268*	0.987*	0.431ns	1451.8	1460.2	9997.8
ARIMA(0, 1, 1)		0.928*	0.479ns	1457.4	1462.9	10653.2
ARIMA(0, 1, 2)		0.755, 0.243	0.430ns	1452.1	1460.4	9919.2
ARIMA(1, 1, 2)	0.141	0.884, 0.113	0.430ns	1453.7	1464.9	9992.8

3.4. Modeling of maximum solar radiation

3.4.1. Arima modeling approach As the series found non-stationary, first difference is required. After first difference, it is converted into stationary form. AR(Φ) and MA(Θ) terms were identified by the correlogram indicated in the Figure 3.6.

Figure 3.6 indicated that *acf* cut-off at lag first, fourth *etc.* and *pacf* cut-off at lag first and second. Therefore, there will be so many models from ARIMA family at different values of p, d and q. Some of them were selected on their performance, which are listed below in Table 3.7

In the above Table 3.7 it clearly indicated that ARIMA(1, 1, 0) model has the significant AR terms and also not vary close to one that means it follows the invertibility condition though its AIC, SBC and MSE are higher compared to other models. Instead of ARIMA(1, 1, 0) some models have

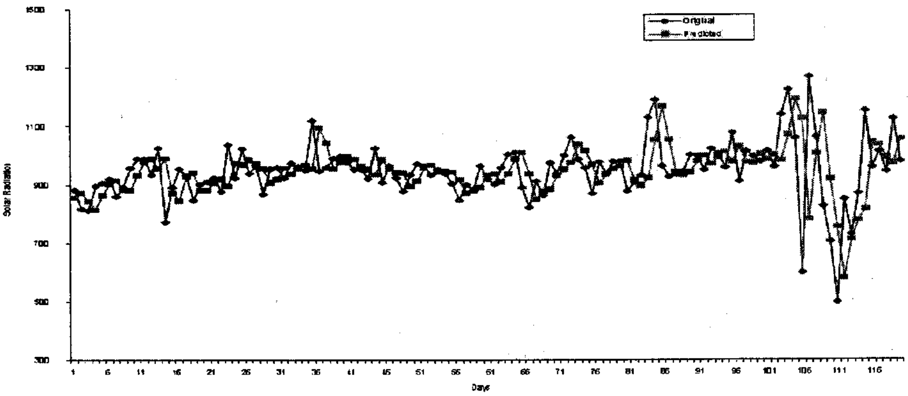

Figure 3.8. Observed and predicted Solar Radiation through Exponential Smoothing Technique

Table 3.8. Fitted Exponential Smoothing models for deviation temperature data

$\alpha = 0.9$			$\alpha = 0.8$			$\alpha = 0.7$		
MSE	K-S Test	Run Test	MSE	K-S Test	Run Test	MSE	K-S Test	Run Test
14234.27	0.103*	2.204*	13364.11	0.110*	2.204*	12646.17	0.121*	2.215*
Bartlett Test for MSE			Not Required due to failure of randomness and normality of residuals					

their coefficients very close to one (failure of invertibility) and some have their coefficients non-significant though their AIC, SBC and MSE are comparatively lower. So the selected model will be ARIMA(1, 1, 0) due to fulfilling of all criteria which we have adopted in this experiment. It graphical representation between observed and expected values is also very close and indicates in the Figure 3.8.

The fitted model for Solar Radiation

$$\hat{Y}_t = C - 0.392Y_{t-1} + \epsilon_i.$$

3.4.2. Exponential Smoothing approach The Exponential Smoothing model also been tried for fitting on the Maximum Solar Radiation data but it could not pass the randomness test as well as the normality test. The results are given in the Table 3.8. The MSE is very large and greater than the ARIMA Models which are the best fitted model for the Maximum Solar Radiation. Bartlett's Test for MSE has not been done for the Exponential Smoothing model because of its failure of the randomness and normality of residuals.

4. Results and Disscussion

As it has been already given in abstract that we have developed the most suitable and closest forecasting models like ARIMA and Exponential Smoothing models using different weather parameters. We have considered Wind speed, Solar Radiation, Maximum Temperature and Deviation Temperature of the Summer Season form March to June month for the Ranchi Region in Jharkhand. The data is taken by own resource with the help of Automatic Weather Station. When we considered the data for maximum temperature we got ARIMA(1, 1, 2) model

$$\hat{Y}_t = C + 0.785Y_{t-1} - 0.559\epsilon_{t-1} - 0.355\epsilon_{t-2} + \epsilon_i$$

is the best fit model on observed and predicted values of maximum temperature which is given in Figure 3.3. The Exponential Smoothing model had also been tried for fitting on the Maximum Temperature data but it could not pass the randomness test as well as the normality test. On considering the data of Observed and Predicted Deviation Temperature we got Exponential Smoothing model

$$\hat{F}_t = 0.9Y_{t-1} + 0.1F_{t-1}$$

is the best fitted model which is given in Figure 3.4. The ARIMA models had also been tried for fitting on the Deviation Temperature data but it could not pass the randomness test as well as the normality test. While analyzing the data of the Wind speed Exponential Smoothing model

$$\hat{F}_t = 0.9Y_{t-1} + 0.1F_{t-1}$$

is best fitted model on the basis of Observed and Predicted values of Wind Speed through Exponential Smoothing Technique given in Figure 3.5. The ARIMA family models had also been tried for fitting on the Wind Speed data but it could not pass the randomness test as well as the normality test. While treating with the data of Solar Radiation again ARIMA model

$$\hat{Y}_t = C - 0.392Y_{t-1} + \epsilon_i$$

is the best fitted model among all the models on the basis of observed and predicted values of Solar Radiation through ARIMA Technique given in Figure 3.7. The Exponential Smoothing model also been tried for fitting on the Maximum Solar Radiation data but it could not pass the randomness test as well as the normality test.

5. Conclusions

Forest fire forecast systems assess the risk of forest fire occurrences. In addition to this, if a fire does take place, it is useful to have assessment of the probability that the fire will become large and erratic. Stability of lower atmosphere plays a key role in this. Conventional stability indexes that indicate the instable and moist atmospheric conditions cannot be used, because the atmosphere in a severe fire event is usually very dry. Consequently, special fire weather indexes may be developed and utilized for future assessment. Here we have proposed an alternative procedure for evaluating the association between derived fire danger indices and fire characteristics that may also be used to estimate, and eventually forecast, frequencies of large fires with known precision. The results indicated that the estimated distribution of fire events agrees reasonably well with those observed.

Similar analyses need to be done with forecasted fire weather/danger indices to assess the skill of the forecasted variables on predicting large fire events in order for this method to be truly useful for fire managers. Future work will address the skill of predicting large fires at different lead times and at smaller temporal and spatial scales using the weather parameters. With fire occurrence data at the individual fire scale and forecasted fire weather/danger indices at the daily and 1 km scale, we should be able to develop forecasts over small regions within administrative units so that the prediction can be used for fire management operation.

Acknowledgements

Authors are thankful to the Ministry of Science & Technology, Govt. of India for providing financial support to carry on experiment on forest fire forecasting system in Jharkhand region. Authors are also thankful to the Birla Institute of Technology, Mesra for providing the entire infrastructure to conduct the experiment.

References

Agee, J. K. and Flewelling, R. (1983). A fire cycle model based on climate for the Olympic Mountains, Washington, In *Proceeding of Fire and Forest Meteorology Conference*, **7**, 32–37.

Anderson, H. E. (1983). Predicting wind-driven wild land fire size and shape, *USDA Forest Service Research Paper INT-305.*

Baker, W. L. (1989a). A review of models of landscape change, *Landscape Ecology*, **2**, 111–133.

Baker, W. L. (1989b). Landscape ecology and nature reserve design in the Boundary Waters Canoe area, Minnesota, *Ecology*, **70**, 23–35.

Baker, W. L. (1992). The landscape ecology of large disturbances in the design and management of nature reserves, *Landscape Ecology*, **7**, 181–194.

Baker, W. L., Egbert, S. L. and Frazier, G. F. (1991). A spatial model for studying the effects of climatic change on the structure of landscapes subject to large disturbance, *Ecological Modelling*, **56**, 109–125.

Bonnicksen, T. M. and Stone, E. C. (1982). Reconstruction of a presettlement giant sequoia-mixed conifer forest community using the aggregation approach, *Ecology*, **63**, 1134–1148.

Box, G. E. P. and Jenkins, G. M. (1976). *Time Series Analysis: Forecasting and Control*, Second Ed., Holden Day, San Francisco.

Brown, J. K., Marsden, M. A., Ryan, K. C. and Reinhardt, E. D. (1985). Predicting duff and woody fuel consumed by prescribed fire in the northern Rocky Mountains, *USDA Forest Service Research Paper INT- 337*, Intermountain Forest and Range Experiment Station, Ogden, Utah.

Burrows, D. A. (1988). *The REFIRES Model: A C Program for Regional Fire Regime Simulation*, Masters Thesis, UC Santa Barbara.

Chou, Y. H., Minnich, R. A., Salazar, L. A., Power, J. D. and Dezzani, R. J. (1990). Spatial autocorrelation of wildfire distribution in the Idyllwild Quadrangle, San Jacinto Mountain, California, *Photogrammetric Engineering and Remote Sensing*, **56**, 1507–1513.

Clark, J. S. (1989). Ecological disturbance as a renewal process: Theory and application to fire history, *Oikos*, **56**, 17–30.

Clark, J. S. (1990). Fire and climate change during the last 750 years in northwestern Minnesota, *Ecological Monographs*, **60**, 135–159.

Fowler, P. M. and Asleson, D. O. (1984). The location of lightning-caused wildland fires in northern Idaho, *Physical Geography*, **5**, 240–252.

Frandsen, W. H. and Andrews, P. L. (1979). Fire behavior in non-uniform fuels, *USDA Forest Service Research Paper*, INT-232, Intermountain Forest and Range Experiment Station, Ogden, Utah.

Green, D. G. (1983). Shapes of simulated fires in discrete fuels, *Ecological Modelling*, **20**, 21–32.

Greig-Smith, P. (1964). *Quantitative Plant Ecology*, Butterworths, London.

Heinselman, M. L. (1973). Fire in the virgin forest of the Boundary Waters Canoe Area, Minnesota, *Quaternary Research*, **3**, 329–382.

Johnson, E. A. and van Wagner, C. E. (1985). The theory and use of two fire history models, *Canadian Journal of Forest Research*, **15**, 214–220.

Kilgore, B. M. (1971). The role of fire in managing red fir forests, *Transactions of the North American wildlife and Natural Resources Conference*, **36**, 405–416.

Kilgore, B. M. (1973). The ecological role of fire in Sierran conifer forests: Its application to national park management, *Journal Quaternary Research*, **3**, 496–513.

Ljung, G. M. and Box, G. E. P. (1978). On A measure of lack of fit in time series models, *Biometrika*, **65**, 297–303.

Makridakis, S., Wheelwright, S. C. and Hyndman, R. J. (2003). *FORECASTING: Methods and Applications* Third Ed., Wiley, Chapter4, pp-136-180.

Martin, R. E. (1982). Fire history and its role in succession, *Forest, Succession and Stand Development in the Northwest*, 92–99.

McKelvey, K. S. and Busse, K. K. (1996). *An evaluation of 20th century fire patterns on forest service lands in the Sierra Nevada*, In Sierra Nevada Ecosystem Project: final report to Congress, vol. II, chap. 41. Davis: University of California, Centers for Water and Wildland Resources.

Meese, R. A. and Geweke, J. (1982). *A Comparison of Autoregressive Univariate Forecasting Procedures for Macroeconomic Time Series*, Unpublished Manuscript, University of California, Berkeley, California.

Minnich, R. A. (1983). Fire mosaics in southern California and northern Baja California, *Science*, **219**, 1287–1294.

Pankratz, A. (1983). *Forecasting with univariate Box-Jenkins Models: Concepts and Cases*, John Wiley & Sons, New York.

Pielou, E. C. (1977). *Mathematical Ecology*, John Wiley & Sons, New York.

Pindyck, R. S. and Rubinfeld, D. L. (1981). *Econometric Models and Economic Forecasts*, 2nd Ed., McGraw-Hill, New York.

Quenouille, M. H. (1949). Approximate tests of correlation in time-series, *Journal of the Royal Statistical Society*, **B11**, 68–84.

Romme, W. H. (1982). Fire and landscape diversity in subalpine forests of Yellowstone National Park, *Ecological Monographs*, **52**, 199–221.

Rossi, R. E., Borth, P. W. and Tollefson, J. J. (1993). Stochastic simulation for characterizing ecological spatial patterns and appraising risk, *Ecological Applications*, **3**, 719–735.

Rothermel, R. C. (1972). A mathematical model for predicting fire spread in wildland fuels, *USDA Forest Service Research Paper*, INT-115

Rothermel, R. C., Wilson, R. A., Morris, G. A. and Sackett, S. S. (1986). Modeling moisture content of fine dead wildland fuels: Input to the BEHAVE fire prediction system. USDA Forest Service Research Paper INT-359, *Intermountain Forest and Range Experiment Station*, Ogden, Utah

Ryan, K. C. and Reinhardt, E. D. (1988). Predicting post-fire mortality of seven western conifers, *Canadian Journal of Forest Research*, **18**, 1291–1297.

Swetnam, T. W. (1993). Fire history and climate change in giant sequoia groves, *Science* **262**, 885–889.

van Wagtentonk, J. W. (1986). The role of fire in the Yosemite wilderness, *Proceedings-National Wilderness Research Conference: Current Research*, USDA Forest Service General Technical Report INT-212, Intermountain Research Station, Ogden, Utah, 2–9.